WATER RESOURCES RESEARCH, VOL. 33, NO. 1, PAGES 247–258, JANUARY 1997

The components of fractional transport rate

Peter R. Wilcock

Department of Geography and Environmental Engineering, Johns Hopkins University, Baltimore, Maryland

Abstract. Fractional transport rates are defined as the product of spatial grain entrainment, displacement length, and displacement frequency. Grain entrainment is defined relative to the population of grains on the bed surface at an initial time in order to account for partial transport, a condition in which only a portion of the exposed grains of a single size D_i are mobilized over the duration of a transport event. A relation for grain displacement frequency is calculated from an assumed relation for displacement length and observed values of fractional transport rate, bed surface size distribution, and spatial entrainment in flume experiments. Fractional transport rates are independent of D_i for fully mobilized fractions and decrease rapidly with D_i for partially mobile fractions; the latter results from a decrease in both the displacement frequency and the mobilized proportion of each fraction. These two terms, which together determine the fractional entrainment rate, have different relations with flow strength and D_i and should be independently included in a general fractional transport model. Grain-size similarity in fractional transport rates does not hold for conditions of partial transport. Partial transport is a grain-scale representation of incipient motion and can be directly related to the reference shear stress τ_{ri}, a surrogate for the critical shear stress for incipient motion based on transport rate rather than grain mobility. Fractional mobilization at different flows may be predicted from τ_{ri}, and partial transport appears to be the general condition at the reference transport rate. Using τ_{ri} as input, the transport component relations are used to predict the bed mobilization and fractional transport rates for a field case.

Introduction

The transport rate of riverbed material can be decomposed into the product of elementary terms, such as grain velocity, displacement distance, and the proportion or rate of grain entrainment. These components arise naturally from the considerations of grain motion used to develop theoretical models of sediment transport. Direct measurements of transport components are needed to extend our understanding of the physics of transport and support the development of general transport models. Such measurements are relatively rare because they require methods quite different from those typically used to measure transport rate. Grain displacements, entrainment rates, and velocities have been measured on motion pictures of the transport of unisize sediment [e.g., *Fernandez Luque and van Beek*, 1976; *Nakagawa et al.*, 1978, 1980; *Nelson et al.*, 1995] and of mixed-size sediment in the laboratory [*Nakagawa et al.*, 1982] and the field [*Drake et al.*, 1988]. Grain entrainment and displacement have also been measured in the field using tracer grains [e.g., *Stelczer*, 1981; *Emmett et al.*, 1990; *Church and Hassan*, 1992; *Hassan et al.*, 1992; *Schmidt and Ergenzinger*, 1992; *Haschenburger*, 1996].

Different sets of transport components can be defined. When observations are made on motion picture film, mass transport rate per unit width $[M\ L^{-1}\ T^{-1}]$ can be decomposed as the product of the spatial concentration $[M\ L^{-2}]$ and velocity $[L\ T^{-1}]$ of moving grains or as the product of the mean length of individual grain displacements $[L]$ and the mass of grains entrained or distrained per unit area and time $[M\ L^{-2}\ T^{-1}]$ under steady state transport conditions. In an unusually complete film analysis of bed load transport, *Drake et al.* [1988] measured both sets of transport components, as well as the flux of grains crossing a flow-normal line, and found all three measures of transport to be consistent. When tracer gravels are used, unit transport rates are calculated as the product of the mean total displacement length $[L]$ over the duration of a transport event $[T^{-1}]$ (typically composed of many individual displacements), the depth $[L]$ of active transport (as measured, for example, with scour chains), the bed porosity, and the grain density $[M\ L^{-3}]$.

Here a different set of transport components is developed in order to account for partial transport, a condition in which only some of the grains exposed on the bed surface are entrained over the duration of a transport event. Partial transport may be defined for the entire population of grains on the bed surface, although it is the partial transport of individual size fractions that is directly relevant to predicting fractional transport rates. In a companion paper [*Wilcock and McArdell*, this issue] we demonstrate the nature and domain of partial transport using direct observations of the immobile proportion of each fraction over the duration of flume experiments with a widely sorted mixed-size sediment. Entrainment of the surface grains within an individual size fraction occurs over a range of bed shear stress τ_0. Within this range that fraction is in a state of partial transport: some grains are active (entrained at least once during a transport event), and the remainder are immobile. We also demonstrate that larger fractions are mobilized at larger flow strengths and that partial transport is associated with a rapid decrease in transport rate with grain size, a tendency noted in many gravel-bed rivers.

To account for partial transport, it is necessary that grain entrainment be specified relative to the grain population present on the bed surface at some initial time. An appropriate

Paper number 96WR02666.
0043-1397/97/96WR-02666$09.00

term is the mass entrainment, over an entire transport event, of the grains found within a particular area at the start of the event. With this approach the proportion of a fraction that is active is considered separately from the frequency of entrainment of the active grains. The spatial entrainment used here may be measured in the field by replacing a volume of the bed with tracer gravels [*Wilcock et al.*, 1996] and recording the proportion or mass of grains removed by the transport event. When this field measure of spatial entrainment is divided by the area of the sample and the duration of the event, the resulting mass entrainment rate will be much smaller than that obtained by directly observing the number of grains entrained per area and time (as with movies). The latter is larger by a factor equal to the mean number of displacements per grain that occur during the event.

In this paper, approximate relations for the individual transport components are developed using observations of fractional transport rate, bed-surface size distribution, and the mobilized proportion of individual size fractions over the duration of flume runs of different flow strength. These relations are used to illustrate the relative contribution of each transport component to the variation of fractional transport rate with grain size and flow strength. The unmodified component relations are then applied to independent transport observations from a gravel-bed river in order to evaluate their general applicability.

Partial transport is a measure of incipient motion based on the proportion of grains entrained at least once during a transport event. An entirely different measure of incipient motion conditions is the reference shear stress τ_{ri}, which is defined as the shear stress that produces a small reference value of a dimensionless transport rate. Because τ_{ri} is defined using transport rates, without regard to the source of the grains, the proportion of the bed surface mobilized under reference transport conditions cannot be determined from the information used to calculate τ_{ri}. One objective of this paper is to demonstrate the degree of bed mobilization associated with τ_{ri}. Because τ_{ri} is easily and commonly determined from typical measurements of transport rate, a means of forecasting the mobilized proportion of the bed at τ_{ri} provides a broader physical interpretation of transport measurements and a basis for estimating the potential grain sorting and sediment exchange between the bed surface and subsurface.

Definition of Transport Components

To account for partial transport, a set of transport components should include a term representing the mobile proportion of each fraction and must, therefore, be referenced to the population of grains on the bed surface at some initial time. To facilitate comparison among different size fractions, flows, and sediments, the individual components should also be defined so that they may be expected to take constant mean values under conditions of steady state transport, so that individual terms do not become arbitrarily large with increasing flow duration or period of observation. An appropriate set of components contains three terms:

$$q_{bi} = M_{ai}(N_t/T)\, L_{1i} \tag{1}$$

where the equation is in units of $[M\ L^{-1}\ T^{-1}]$, M_{ai} is the mass of fraction i entrained per unit bed area over the time period T $[M\ L^{-2}\ T^{-1}]$, N_t is the number of times an individual grain of fraction i is entrained during T, and L_{1i} is the mean length of a single displacement. M_{ai} is defined to include only grains found within an area of the bed at the start of T. Other grains, with an initial position outside of the area, will be deposited and reentrained during T. The total mass of sediment, regardless of its initial position, that is entrained from unit bed area over T will be larger than M_{ai} by a factor of N_t.

Although all variables in (1) can be represented by frequency distributions, the focus here is their mean values, as defined in (1). The product of means given in (1) is equivalent to the ensemble average product for some plausible frequency distributions of the transport components (e.g., an exponential or gamma distribution for L_{1i}, as suggested by *Einstein* [1937], and recently evaluated using tracer gravels by *Hassan and Church* [1992] and *Schmidt and Ergenzinger* [1992]). For other possible frequency distributions for the transport components the transport components in (1) must be regarded as "effective" averages, in the sense that they are defined such that their product gives the mean q_{bi} (D. Furbish, personal communication, 1996).

Under steady state transport conditions, q_{bi} fluctuates about a constant mean. The transport components in (1) are defined so that the time average of all terms on the right-hand side approaches a constant value under steady state conditions. M_{ai} may be expected to increase with time over an initial period during which the active grains are entrained and then approach a constant value as the number of remaining entrainable grains approaches zero. The duration of this initial period presumably corresponds to both the duration and strength of the flow, suggesting that it should scale with the cumulative mass of transported sediment. The rate at which additional grains are entrained from an initial bed surface becomes approximately zero after the cumulative transport of approximately two to four surface layers [*Wilcock and McArdell*, this issue]. The time average of L_{1i} may be expected to approach a constant value once the bed and transport reach a mutual adjustment under steady state conditions. In contrast, N_t may be expected to increase directly with time, so it is the appropriate term in (1) to be scaled by T.

Experimental Observations

The experimental observations used here to develop specific functional relations for the components in (1) were collected from flume runs using a range of flow strengths and a widely sorted sand/gravel mixture [*Wilcock and McArdell*, 1993; this issue]. The sediment has a bimodal grain-size distribution with a minimum size of 0.21 mm, median size D_{50} = 5.3 mm, and maximum size of 64 mm. The experimental runs span a range in mean bed shear stress τ_0 from 2.0 to 7.3 Pa and a range in transport rate q_b from 7.5 to 570 g m^{-1} s^{-1}.

The relevant measurements include the transport rate of individual size fractions q_{bi}, the proportion of each fraction on the bed surface F_i, and the proportion of each fraction mobilized over the duration of each run Y_i. The latter was determined from time series of photographs of the bed surface. Grain immobility observations were made for all size fractions coarser than 4.0 mm, which includes the coarsest 58% of the sediment. The results of four of five runs with grain immobility observations are presented here; the omitted run has a shear stress and transport rate similar to one of the included runs but a shorter duration, so that the estimates of Y_i are less certain. Detail regarding the experimental methods and the variation

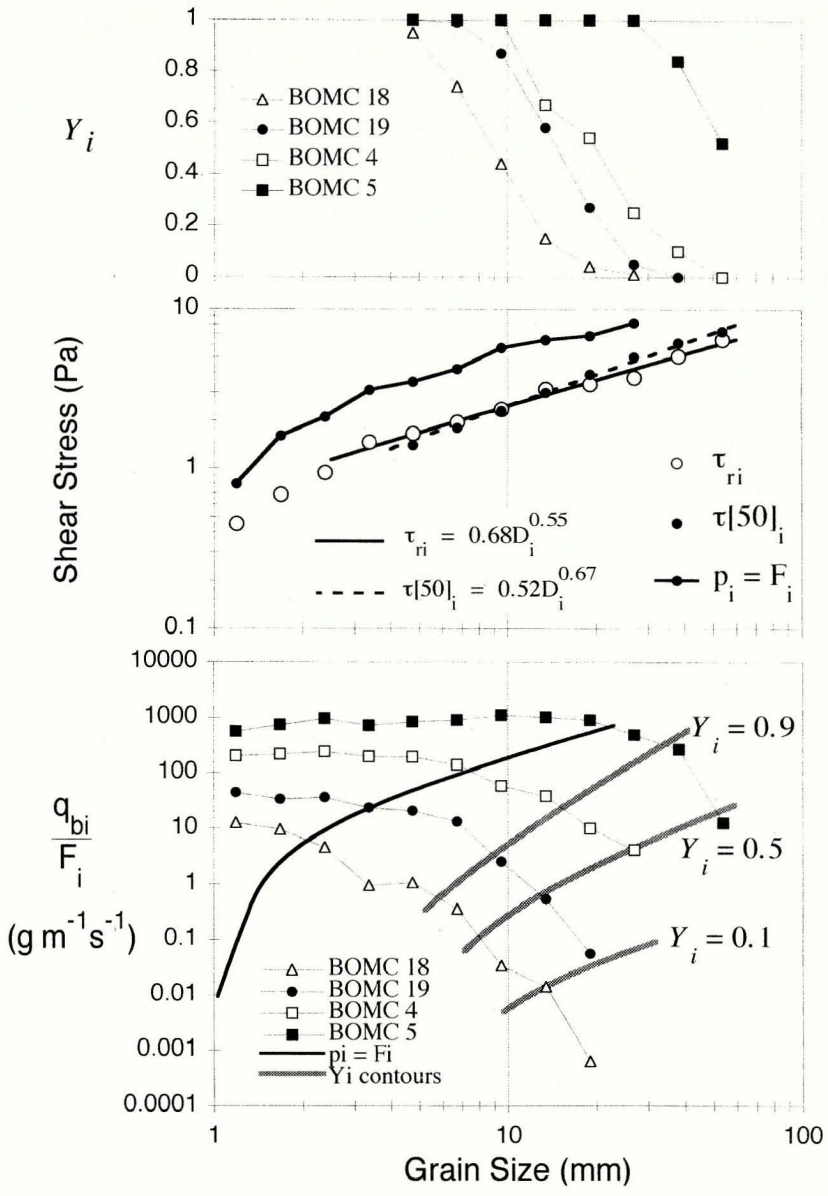

Figure 1. Summary of grain immobility and fractional transport observations, as a function of grain size D_i, for the BOMC sediment [*Wilcock and McArdell*, this issue]. (a) Mobile proportion Y_i of individual size fractions. (b) Reference shear stress τ_{ri}, shear stress ($\tau[50]_i$) that mobilizes 50% of individual size fractions, and shear stress producing equal mobility ($p_i = F_i$). (c) Fractional transport rates q_{bi}/F_i, with contours of $Y_i = 0.1$, 0.5, and 0.9 superimposed. Values of mean bed shear stress τ_0 and total transport rate q_b for each run are BOMC18: 2.0 Pa, 7.5 g m^{-1} s^{-1}; BOMC19: 3.2 Pa, 25.7 g m^{-1} s^{-1}; BOMC4: 5.0 Pa, 157 g m^{-1} s^{-1}; and BOMC5: 7.3 Pa, 572 g m^{-1} s^{-1}.

of Y_i with bed shear stress τ_0 and grain size D_i, which demonstrates the nature and domain of partial transport, are given in a companion paper [*Wilcock and McArdell*, this issue]. The salient results of these experiments are summarized in Figure 1 and are briefly described here.

The mobile proportion of each fraction on the bed surface Y_i decreases with grain size D_i and increases with bed shear stress τ_0 (Figure 1a). The distribution of Y_i for each D_i can be approximated by a lognormal distribution of $\tau_0/\tau[50]_i$, where $\tau[50]_i$ is the value of τ_0 producing $Y_i = 0.5$. A standard deviation of 0.2 can be used to approximate the Y_i distribution for each fraction, yielding the result that the transition $0.1 < Y_i < 0.9$ occurs over a range in τ_0 of a factor of 2 for each size; $\tau[50]_i$ was found to increase consistently with grain size (Figure 1b) so that at a particular τ_0, the range of sizes in a state of partial transport is between a factor of 2 and 4.

The stress $\tau[50]_i$ producing $Y_i = 0.5$ is closely related to the reference shear stress τ_{ri}, which is determined as the value of τ_0 producing a small reference value of the dimensionless transport rate

$$W_i^* = \frac{(s-1)gq_{bi}}{F_i\rho_s u_*^3} \tag{2}$$

where ρ_s is the sediment density; s is the relative sediment density ρ_s/ρ; g is the acceleration of gravity; u_* is the shear velocity, given by $(\tau_0/\rho)^{1/2}$; and the reference transport rate is $W_i^* = 0.002$. For the experimental sediment, $\tau_{ri} \propto D_i^{0.55}$ for sizes coarser than 2.8 mm ($\approx D_{37}$) [*Wilcock and McArdell*,

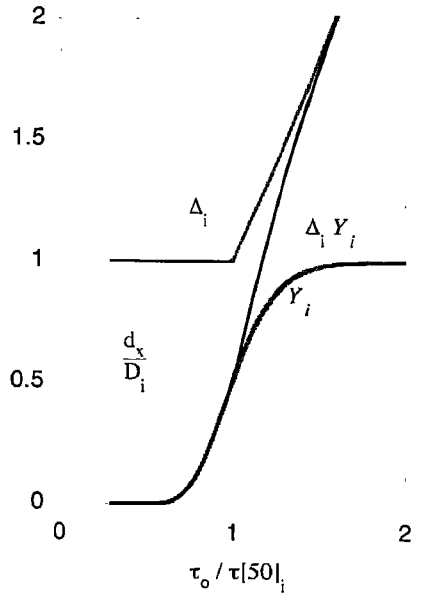

Figure 2. Variation with $\tau_0/\tau[50]_i$ of Y_i, Δ_i, and their product ($\Delta_i Y_i$). Y_i calculated as a lognormal distribution of $\tau_0/\tau[50]_i$ with mean 0.0 and standard deviation 0.2. Δ_i calculated using (7) with d_x calculated from (8) for $Y_i > 0.5$.

1993], which is a much stronger variation with D_i than that commonly reported for mixed-size sediments and has been attributed to the widely sorted, bimodal nature of the size distribution [*Wilcock*, 1993]. The active proportion of a fraction at τ_{ri} decreases from $Y_i \approx 0.8$ for D_{50} to $Y_i = 0.2$ for fractions larger than 22.6 mm ($\approx D_{80}$). As a result, $\tau[50]_i \propto D_i^{0.67}$ (Figure 1b), a trend similar to but steeper than that for τ_{ri}. The relation between $\tau[50]_i$ and D_i may be inverted to give the grain size $D[50]_i$ that is 50% mobilized at a particular τ_0 as $D[50]_i \propto \tau_0^{1.5}$ (a similar exponent is derived from direct regression of D_i on $\tau[50]_i$).

The scaled fractional transport rates q_{bi}/F_i decrease rapidly with grain size for fractions in a state of partial transport (Figure 1c). Complete mobilization of a fraction ($Y_i = 1$) occurs within 1 order of magnitude in transport rate of equal mobility in transport rates, defined as an equal proportion of a fraction on the bed surface F_i and in transport p_i. The decrease of q_{bi}/F_i with D_i may be attributed either to a decrease in the proportion of active grains in a size fraction or to a decrease in the displacement frequency of active grains [*Wilcock and McArdell*, 1993]. One objective here is to evaluate the relative contribution of each transport component to the fractional transport rate.

Approximation of Transport Components

In the following, M_{ai} is estimated using experimental observations of Y_i and the bed surface size distribution F_i. Of the two remaining transport components, neither N_i/T nor L_{1i} were measured, but one of these may be calculated using (1) and measured values of q_{bi}/F_i, if a function of τ_0 and D_i can be specified for the other. Because some independent observations of L_{1i} are available, a function for L_{1i} is assumed and N_i/T is calculated from (1).

Entrainment

The number of grains of size i per unit bed area is approximately F_i/D_i^2. Multiplying this by Y_i and the mass of an individual grain m_i gives the mass entrainment, per unit area, from the bed surface:

$$M_{ai} = (m_i F_i Y_i / D_i^2) \tag{3}$$

where the equation is in units of $[M\,L^{-2}]$. Because it represents entrainment from only the bed surface, (3) is likely to underestimate the entrainment of finer fractions at flows larger than those causing full mobilization ($Y_i = 1$). In this case, subsurface grains will also be entrained and M_{ai} becomes proportional to an exchange depth d_x. For $Y_i = 1.0$, M_{ai} is given by

$$M_{ai} = (m_i F_i / D_i^3)\, d_x \tag{4}$$

where the term in parentheses represents the mass of fraction i per unit volume of bed which when multiplied by d_x, gives the mass of fraction i entrained per unit bed area. Here d_x is approximated as the size of the fraction $D[50]_i$ that is 50% mobile at a given τ_0. For the experimental sediment a suitable dimensionless form for this relation [*Wilcock and McArdell*, this issue] is

$$d_x/D_{50} = 397(\tau^*_{50})^{1.5} \tag{5}$$

where τ^*_{50} is the Shields parameter $\tau_0/[(s-1)\rho g D_{50}]$. Because $D[50]_i$ and d_x depend on the incipient motion conditions for individual size fractions, which can vary with sediment properties [e.g., *Wilcock*, 1993], the form of (5) is likely to be particular to our experimental sediment. The basis for a more general calculation of d_x from observed values of τ_{ri} is developed later in this paper.

For $d_x \le D_i$, a condition of partial transport may be assumed to exist and M_{ai} is given by (3). For d_x much greater than D_i, a fraction may be assumed to be fully mobilized ($Y_i = 1$) and M_{ai} is given by (4). A smooth transition between the two is achieved using the fact that $d_x = D[50]_i = D_i$ at $Y_i = 0.5$ and specifying M_{ai} as

$$M_{ai} = \left(\frac{\pi}{6}\rho_s\right) F_i D_i \Delta_i Y_i \tag{6}$$

where Δ_i is given by

$$\Delta_i = \begin{cases} 1 & Y_i \le 0.5 \\ d_x/D_i & 0.5 < Y_i \le 1.0 \end{cases} \tag{7}$$

and a spherical grain volume is assumed, giving $m_i = (\pi/6)\rho_s D_i^3$. The variation with $\tau_0/\tau[50]_i$ of Y_i, Δ_i, and their product is shown in Figure 2. Y_i is given by a lognormal distribution of $\tau_0/\tau[50]_i$ with mean zero and standard deviation 0.2; d_x/D_i is given by (5), which, using the fact that $d_x = D_i$ at $\tau_0 = \tau[50]_i$, may be expressed as

$$d_x/D_i = (\tau_0/\tau[50]_i)^{1.5} \tag{8}$$

For later purposes we note that Δ_i differs from d_x/D_i by no more than a factor of 2 for $Y_i > 0.01$, so that $\Delta_i \approx d_x/D_i$ provides a useful approximation for all measurable grain entrainment.

Displacement Length

The mean length of individual grain displacements L_{1i} may be expected to depend on both τ_0 and D_i. *Schmidt and Ergen-*

zinger [1992] used radio tracers in a steep mountain stream and found that L_{1i} for discharges greater than the mean observed during their field work were nearly twice those for discharges smaller than the mean. *Nakagawa et al.* [1982] calculated L_{1i} for individual fractions in mixed-size sands using observed q_{bi} and displacement frequencies (comparable to N_i/T) measured from motion picture film. They proposed a relation for displacement length in which L_{1i} is proportional to $(\tau_0)^{1/2}$. Although their calculated values of L_{1i} clearly increase with τ_0, the scatter in the data and the limited range of τ_0 used in their experiments prevented a general confirmation of this relation. Nakagawa et al. also found that L_{1i} increased directly with D_i, so that L_{1i}/D_i took values between 6 and 30, where some of the variation is explained by τ_0.

Visual observations of L_{1i} in a laboratory flume were made for a range of flows and a single grain size (D = 33 mm) by *Stelczer* [1981, p. 194], who found that L_{1i} varied directly with the near-bed flow velocity u_f over a 5-fold range in u_f (0.2–1.0 m s^{-1}). Assuming a standard logarithmic velocity profile in the near-bed region, L_{1i} is then proportional to the square root of τ_0, as proposed by *Nakagawa et al.* [1982].

The most detailed observations of displacement length in a mixed-size sediment have been made by *Drake et al.* [1988], who directly measured L_{1i} on motion picture film of transport on Duck Creek, a gravel-bed stream with D_{50} = 4.0 mm. They measured L_{1i} for three sizes, 2–4, 4–8, and 8–16 mm, and found L_{1i} to be given approximately by 15 D_i. The films were made at a constant flow strength corresponding to τ^*_{50} = 0.093, so the variation of L_{1i} with τ_0 could not be determined. This value of τ^*_{50} is bracketed by the values used in the experiments of *Nakagawa et al.* [1982] ($0.032 < \tau^*_{50} < 0.15$ for runs with five different sediments). The result of Drake et al. may be combined with a square root dependence on τ_0 in the dimensionless form

$$L_{1i}/D_i = 15(\tau^*_{50}/0.093)^{0.5} \tag{9}$$

A larger coefficient in (9), on the order of 60, is needed to fit the *Stelczer* [1981] data, although a direct comparison cannot be made because Stelczer's results are given in terms of the bottom velocity u_f, rather than τ_0. The difference between the two constants may be attributed in part to a decrease in L_{1i} for the widely sorted mixture in the field case. Further, it is likely that real-time observation of tracer displacement lengths will be biased toward longer displacements, whereas film analysis facilitates the measurement of displacements of short length. Because of the greater accuracy of film observations and the widely sorted nature of the field sediment, the value of 15 is used in (9) and the absolute error in this estimate of L_{1i} is assumed to be no larger than a factor of 4. The relative error in L_{1i} from size to size should be smaller.

Most observations and estimates of L_{1i} are for sizes in the coarser half of the grain-size distribution, so little information is available to estimate L_{1i} for D_i much smaller than D_{50}. Although the focus here is also on the coarse half of the size distribution, a means of estimating L_{1i} for $D_i < D_{50}$ is useful in order to estimate fractional transport rates for the entire bed size distribution. If L_{1i} for the finer fractions is influenced by both the absolute grain size D_i and the general roughness field of the bed surface, a plausible modification of (9) is

$$\frac{L_{1i}}{D_i} = 15\left(\frac{D_i}{D_{50}}\right)^{\xi}\left(\frac{\tau^*_{50}}{0.093}\right)^{0.5} \tag{10}$$

where $(D_i/D_{50})^{\xi}$ accounts for the relative size effect on L_{1i}.

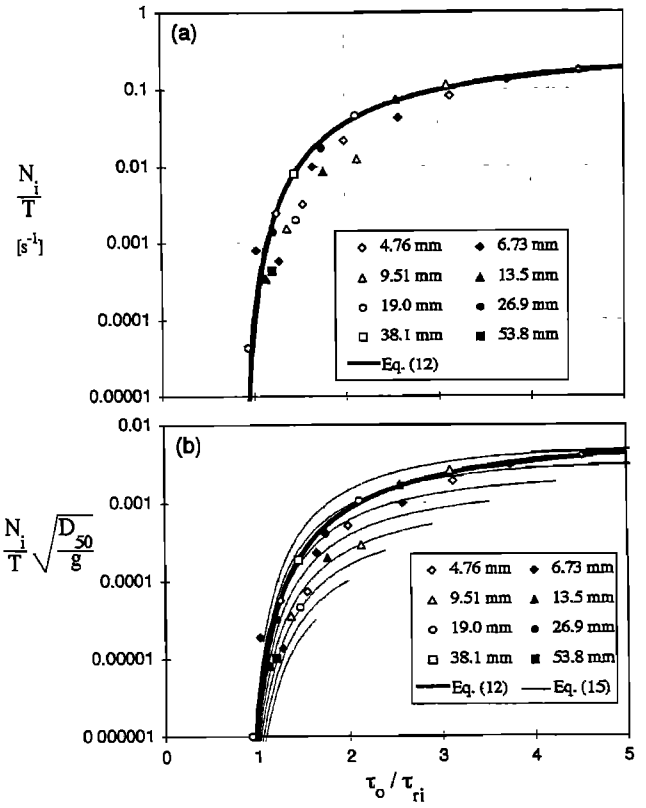

Figure 3. Calculated values of (a) displacement frequency N_i/T and (b) dimensionless displacement frequency N^*_i, as a function of τ_0/τ_{ri}. N_i/T calculated from (1), using (5), (6), (7), and (9). Single curve in each panel is (12); multiple curves in Figure 3b are fractional values of N^*_i from (15). Scaling τ_0 by τ_{ri} provides a similarity collapse for N_i/T and N^*_i.

The range of ξ may fall between zero ($L_{1i} \propto D_i$) and -1 (for which L_{1i} is entirely determined by bed roughness, represented by D_{50}). $(D_i/D_{50})^{\xi}$ adds a parameter to the formulation that can only be adjusted by comparing predicted and observed fractional transport rates, although it will be shown later that its effects on the variation of q_{bi}/F_i with D_i are relatively limited. Equation (10) is applied only to fractions finer than D_{50}; (9) is used for the coarser fractions.

Displacement Frequency

N_i/T may be calculated from (1) using measured values of q_{bi}, F_i, τ_0, and Y_i with (5), (6), (7), and (9). Calculated values of N_i/T are plotted in Figure 3a as a function of τ_0/τ_{ri}. The narrow scatter of the data suggests that N_i/T is independent of grain size beyond its effect on τ_{ri}. The collapse produced by τ_0/τ_{ri} is superior to that produced by $\tau_0/\tau[50]_i$, which may be expected because τ_{ri} is determined as the value of τ_0 associated with a particular transport rate and q_{bi} is the dominant term producing the variation in the N_i/T estimated from (1). The absence of size dependence in Figure 3a suggests that a suitable dimensionless form for N_i/T is

$$N^*_i = \frac{N_i}{T}\left(\frac{D_{50}}{g}\right)^{1/2} \tag{11}$$

which is plotted as a function of τ_0/τ_{ri} in Figure 3b.

It is useful to represent the trend between N^*_i and τ_0/τ_{ri} with

a closed-form function in order to illustrate the relations among the different components of fractional transport and to compare the transport components with existing transport relations. If there is no size dependence in this relation (i.e., all size dependence is accounted for by τ_{ri}), a single relation may be fitted to all grain sizes on Figure 3. The relation

$$N_i^* = K\left[1 - 0.85\,\frac{\tau_{ri}}{\tau_0}\right]^{4.5} \qquad (12)$$

with $K = 0.01$ is shown in Figure 3b. The relation shown in Figure 3a differs from (12) by the factor $(g/D_{50})^{1/2}$. The form of (12) is suggested by the transport relation of *Parker* [1979]:

$$\frac{W_i^*}{W_r^*} = 5600\left[1 - 0.85\,\frac{\tau_{ri}}{\tau_0}\right]^{4.5} \qquad (13)$$

where W_i^* is the dimensionless transport rate defined in (2) and W_r^* is the reference transport rate, taken to be 0.002. Equation (13) is a power approximation of the Einstein transport relation at small transport rates and has been found to represent gravel-bed transport rates measured under a variety of conditions. Using (12) to represent N_i^* facilitates a comparison in a later section of the transport components developed here with those implied by a similarity collapse of fractional transport rates, of which (13) is one example.

Comparison of Transport Components

The components of fractional transport rate are presented in Figure 4 as a function of grain size, which provides the most direct illustration of partial transport and the decrease in transport rate with grain size. M_{ai}/F_i is found from (5), (6), and (7), with Y_i given by a lognormal distribution of $\tau_0/\tau[50]_i$ and the values of $\tau[50]_i$ in Figure 1b. N_i/T is found from (12), and L_{1i} is found from (9) for $D_i > D_{50}$ and from (10) for $D_i < D_{50}$. Observed q_{bi}/F_i is shown together with the values calculated from (1) using the plotted transport components. Values are shown for all size fractions, even though the immobility observations and the relation for N_i/T are developed for sizes coarser than 4.0 mm.

Observed and predicted values of q_{bi}/F_i match closely, which is no real measure of predictive capability because N_i/T has been calculated from the observed transport, but does indicate that the component functions provide a consistent representation for all D_i and τ_0. For $D_i < D_{50}$, two values of the parameter ξ in (10) are shown: $\xi = 0$, making (10) identical to (9); and $\xi = -0.3$, causing L_{1i} to decrease less rapidly with decreasing D_i. The differences in L_{1i} and q_{bi}/F_i for these two estimates are relatively minor; $\xi = -0.3$ causes q_{bi}/F_i to decrease less rapidly with D_i and therefore may provide a slightly better representation of L_{1i} for smaller D_i.

Figure 4 illustrates the effect of partial transport on fractional transport rates. M_{ai}/F_i is independent of D_i for $Y_i = 1$ and decreases rapidly over the partial transport range as Y_i decreases to zero over a range in grain size of approximately a factor of 4. N_i/T increases with decreasing grain size, driven by the decrease in τ_{ri} and corresponding increase in τ_0/τ_{ri}. L_{1i} increases with D_i and increases slightly with τ_0. In the fully mobilized region of transport the variation with D_i of L_{1i} and N_i/T roughly balance to produce approximate equal mobility, shown as a weak variation of q_{bi}/F_i with D_i. In the partial transport region, M_{ai}/F_i decreases rapidly with grain size, taking the same sign as N_i/T, and the fractional transport rates decrease rapidly to vanishingly small values. This suggests that the characteristic decrease in transport rate with grain size in gravel-bed rivers results from a corresponding decrease in both the proportion of active grains and their displacement frequency.

Exchange Rates

The mean rate of grain entrainment per unit bed area (regardless of grain position at some initial time) may be directly measured on motion picture film [e.g., *Fernandez Luque and van Beek*, 1976; *Drake et al.*, 1988]. This may be called the exchange rate E_{ai} to distinguish it from the entrainment rate M_{ai}/T. Drake et al. measured E_{ai} from motion picture film for three size fractions and a constant flow strength. Values of E_{ai} may be calculated for the BOMC runs as $M_{ai}(N_i/T)$, providing a comparison with the results of Drake et al. and (because τ_0 is varied in the BOMC runs) an illustration of the possible variation of E_{ai} with both D_i and τ_0.

Because E_{ai} will depend on the proportion of each fraction available for entrainment, comparison among different sediments requires scaling by F_i. *Drake et al.* [1988] measured the bed surface composition as a mass concentration $C_{bi}[M\,L^{-2}]$ rather than as a proportion, because the proportion of the finest fractions could not be reliably determined on the film. The scaled exchange rate is therefore the proportion of surface grains entrained per unit time $E_{pi} = E_{ai}/C_{bi}[T^{-1}]$. This is equivalent to the product $Y_i(N_i/T)$ and values of E_{pi} calculated for BOMC are compared to those observed for Duck Creek in Figure 5.

To facilitate the comparison, E_{pi} is plotted as a function of relative grain size D_i/D_{50} and values of the dimensionless transport rate $q_{50}^* = q_{bi}/\{\rho_s[(s-1)\,gD_{50}^3]^{0.5}\}$ are indicated for each BOMC run. The value of q_{50}^* for the Duck Creek data is 0.003 for the mean transport rate of approximately 8 g m^{-1} s^{-1}. The transport rate (calculated as $E_{ai}L_{1i}$) in the frames used for measuring E_{ai} is 50–100% larger, so the BOMC run with comparable transport rates is BOMC19, for which $q_{50}^* = 0.0062$. Values of E_{pi} for Duck Creek are also calculated using observed q_{bi} and L_{1i} and $E_{pi} = q_{bi}/(L_{1i}C_{bi})$. These values are smaller than those found directly from the measured E_{ai} because the mean transport rate is smaller than that in the portion of film used to measure E_{ai}. Values of E_{pi} agree relatively closely for the two finer sizes at Duck Creek, and the largest size deviates somewhat (Figure 5). The similar order of magnitude for the Duck Creek and BOMC E_{pi} is significant, given the very different means by which E_{pi} is estimated. Detail of the variation of E_{pi} with D_i is likely to be influenced by the size distribution in each case. In particular, a weaker variation of E_{pi} with D_i may be expected for the narrower size distribution in the field case.

For the BOMC values, E_{pi} decreases rapidly with grain size, primarily as a function of decreasing N_i/T for all sizes and decreasing Y_i for the coarsest few fractions (Figure 4). For

Figure 4. (opposite) Components of fractional transport rates for runs (a) BOMC18, (b) BOMC19, (c) BOMC4, and (d) BOMC5. Method of calculation explained in text. The grain size D_{ref} that is just at reference transport conditions for each run is found from $\tau_{ri} = 0.68D_i^{0.55}$. Calculated values shown for $L_{1i} \propto D_i$ for all D_i (9) and for $L_{1i} \propto D_i^{0.7}$ for $D_i < D_{50}$ ($\xi = -0.3$ in (10)). The latter provide a slightly better fit to q_{bi}/F_i. Calculated and observed transport rates match closely for sizes smaller than 4.0 mm, for which no immobility observations were made and which were not used to fit (12).

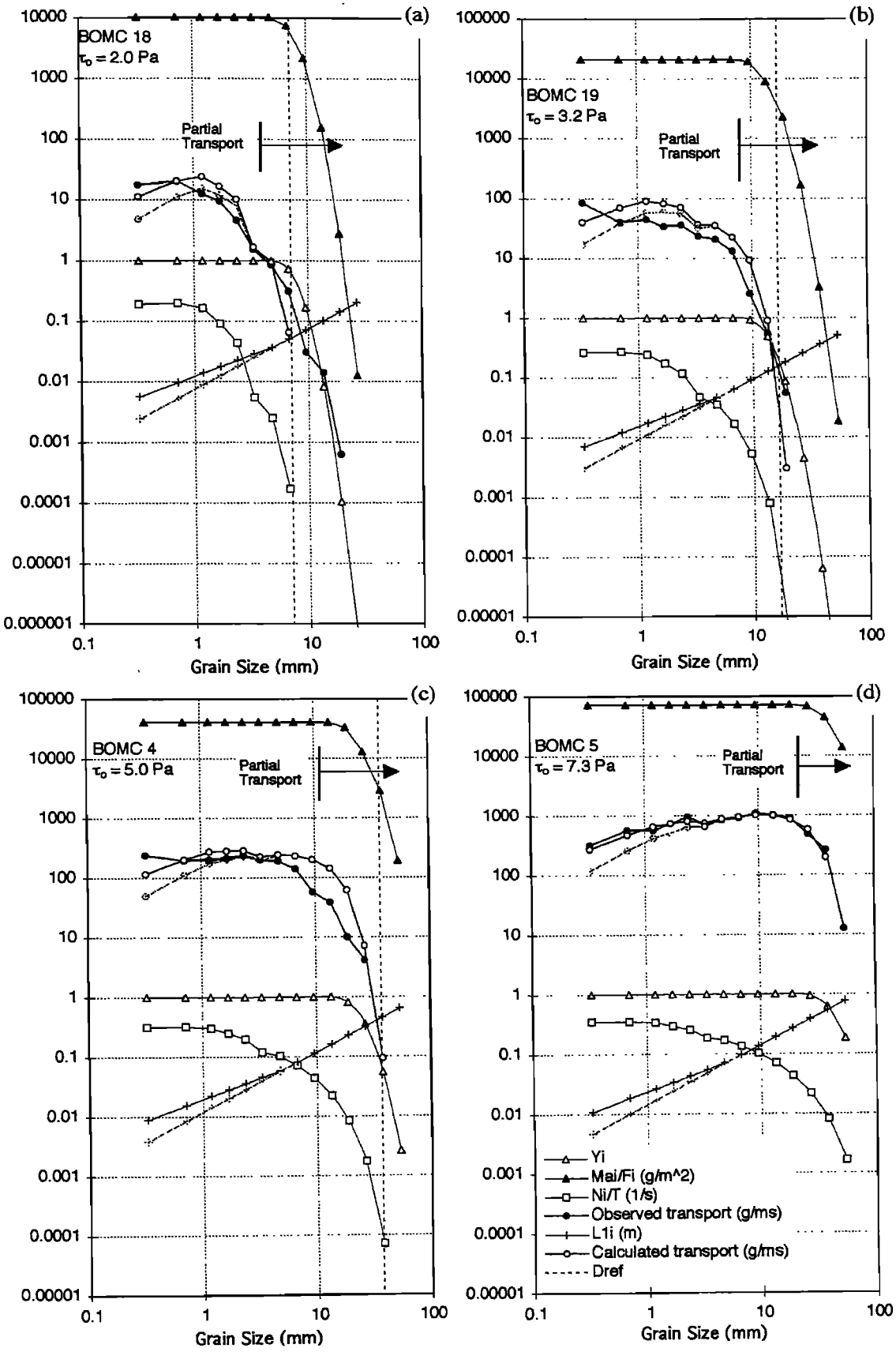
(a)
BOMC 18
τ_o = 2.0 Pa
Partial Transport
Grain Size (mm)
(b)
BOMC 19
τ_o = 3.2 Pa
Partial Transport
Grain Size (mm)
(c)
BOMC 4
τ_o = 5.0 Pa
Partial Transport
Grain Size (mm)
(d)
BOMC 5
τ_o = 7.3 Pa
Partial Transport
Grain Size (mm)
Yi
Mai/Fi (g/m^2)
Ni/T (1/s)
Observed transport (g/ms)
L1i (m)
Calculated transport (g/ms)
Dref

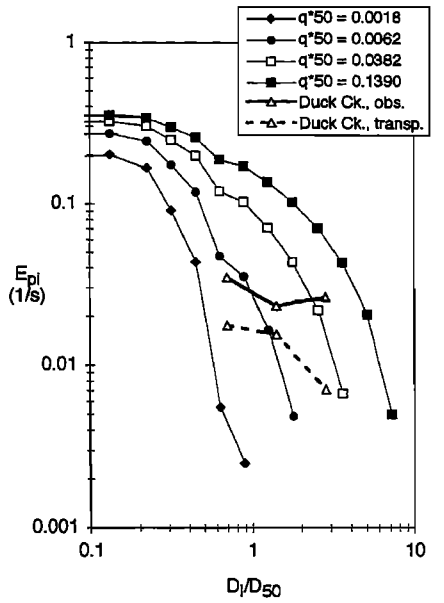

Figure 5. Proportional exchange rate E_{pi} as a function of grain size D_i. BOMC values calculated as $Y_i(N_i/T)$. Duck Creek values obtained from measurements on motion picture film of (1) exchange rate E_{ai} and bed concentration C_{bi} ("obs.") and (2) fractional transport rates and displacement lengths L_{1i} ("transp."). The BOMC run with the transport conditions closest to those of Duck Creek is BOMC19, for which $q^*_{50} = 0.0062$.

fully mobilized grains, E_{pi} increases with flow strength from 0.2 to 0.35 s^{-1} over the range of transport rates measured with BOMC.

Similarity of Fractional Transport Rates

In the *Parker* [1979] transport relation (13), W_i^* is independent of D_i beyond its influence on τ_{ri}. This is the classic similarity transformation for fractional transport rates found in earlier mixed-size sediment transport models [e.g., *Ashida and Michue*, 1972; *Parker et al.*, 1982]. In this approach the form of the transport relation (such as (13)) is taken to be independent of grain size, because size-dependent differences in fractional transport rate are assumed to be entirely accounted for by the variation of τ_{ri} with D_i.

The transport component relations developed here may be compared to the similarity hypothesis by using (1), (6), (9), and (12) in the definition of W_i^* (2) to develop an alternative expression for W_i^*:

$$\frac{W_i^*}{W_r^*} = 5100\left(\frac{Y_i}{Y_n}\right)\left(\frac{d_x}{d_{xr}}\right)\left(\frac{\tau_n}{\tau_0}\right)\left[1 - 0.85\,\frac{\tau_n}{\tau_0}\right]^{4.5} \qquad (14a)$$

where Y_{ri} and d_{xr} are the values of Y_i and d_x at the reference transport rate and Δ_i is assumed to equal d_x/D_i for all Y_i. If $d_x \propto \tau_0^{\beta}$, as in (8), (14a) may be reduced to

$$\frac{W_i^*}{W_r^*} = 5100\left(\frac{Y_i}{Y_n}\right)\left(\frac{\tau_0}{\tau_n}\right)^{\beta-1}\left[1 - 0.85\,\frac{\tau_n}{\tau_0}\right]^{4.5} \qquad (14b)$$

This expression for W_i^* contains an explicit size dependence in the term Y_i, suggesting that partial transport causes a systematic deviation from similarity in fractional transport rates.

The inverse case is also illustrative. An expression for N_i^* can be developed from (13) using the component relations for M_{ai} and L_{1i}. After considerable manipulation using (1), (2), (5), (6), (7), and (9) in (13), the result is

$$N_i^* = \frac{1}{327(D_i/D_{50})(\tau^*_{50})^{1/2}}\left[1 - 0.85\,\frac{\tau_{ri}}{\tau_0}\right]^{4.5} \qquad (15)$$

where the constant 327 is chosen to make the resulting fractional entrainment curves fall about the data in Figure 3b. This constant corresponds to a constant in (13) of $12{,}150Y_i$, rather than 5600. If W_i^*/W_r^* is taken to be independent of D_i (transport similarity), then a size dependence in N_i^* is implied by the component relations for M_{ai} and L_{1i}. This size dependence is not evident in the calculated values of N_i^* (Figure 3b). If N_i^* is taken to be independent of grain size, then W_i^*/W_r^* will have a size dependence for partially mobile fractions, as in (14).

Relation Between Partial Transport and the Reference Transport Rate

The calculated transport components in Figure 4 depend on two essential empirical results: the variation with D_i of $\tau[50]_i$ and τ_{ri}. The first determines the degree of partial transport and the entrainment per unit area of each fraction; the second is used to scale τ_0 in the prediction of the displacement frequency. Although both measures of incipient motion show a similar variation with D_i, each was measured independently and by different methods. Because $\tau[50]_i$ is not generally known, whereas τ_{ri} may be measured or estimated, the goal here is to develop a relation between the two, so that $\tau[50]_i$ may be predicted as a function of τ_{ri}. This provides a basis for not only predicting the degree of partial transport at the reference transport rate but also for calculating the transport components for other sediments with known τ_{ri}.

The transport component relation (1) may be substituted in the definition of W_i^* (2) so that the reference transport definition becomes

$$\frac{(s-1)g}{\rho_s u_*^3}\left(\frac{M_{ai}}{F_i}\right)_r\left(\frac{N_i}{T}\right)_r (L_{1i})_r = 0.002 \qquad (16)$$

where the r subscript denotes values at reference transport conditions. If N_i/T is assumed to be a function of only τ_0/τ_{ri}, as suggested by (12) and Figure 3b, N_i/T will be a constant at the reference transport rate, for which $\tau_0/\tau_{ri} = 1$. With this assumption and using (6) to represent M_{ai}/F_i, (16) may be solved for Y_i at the reference transport rate, Y_{ri}, giving

$$Y_n = \text{const}\,[\tau_n^{1.5}/D_i(\Delta_i)_r(L_{1i})_r] \qquad (17)$$

where const includes all numerical constants and terms related to g, ρ, and ρ_s. The variation of Y_{ri} with D_i can be approximated by assuming that $\tau_{ri} \propto D_i^{\theta}$ (where θ is a constant) and that the denominator in (17) is proportional to D_i^2 ($L_{1i} \propto D_i$ from (9) and, at the reference transport rate, $(\Delta_i)_r \approx 1.0$). For $0 < \theta < 0.67$, which should represent nearly all sediments, (17) becomes $Y_{ri} \propto D_i^{\gamma}$, with $-1 < \gamma < -2$ and γ becoming more negative as θ approaches zero. Thus Y_{ri} is found to decrease with grain size, using no result specific to the BOMC sediment except that N_i/T is assumed to be a function of only τ_0/τ_{ri}. Because Y_{ri} must be less than or equal to 1, a decrease of Y_{ri} with grain size implies that partial transport exists at reference transport conditions.

For the specific functions (6, 9, and 12) used here to approximate the transport components, solving (16) for Y_{ri} gives

$$Y_{ri} = 39.6(s-1)^{1/2}\frac{\tau_{ri}^*}{(\Delta_i)_r(D_i/D_{50})} \qquad (18)$$

where $\tau_{ri}^* = \tau_{ri}/[(s-1)\rho g D_i]$. Because $\tau_{ri} \propto D_i^{0.55}$ for the BOMC sediment, (18) shows that Y_{ri} varies with D_i to approximately the $-3/2$ power. Values of Y_{ri} calculated using observed τ_{ri} in (18) are shown in Figure 6a together with values determined directly from the grain immobility observations [*Wilcock and McArdell*, this issue, Figure 3b]. The agreement between the two is quite good. For the BOMC sediment, (18) may be used to predict Y_{ri} from specified values of τ_{ri} and D_i/D_{50}. It remains to be demonstrated that this relation is accurate for other sediments.

A relation between τ_{ri} and Y_{ri} may also be developed from the *Parker* [1979] transport relation. At $\tau_0 = \tau_{ri}$, the ratio W_i^*/W_r^* on the left side of (13) is equal to 1. If the constant 5600 in (13) is replaced by $12{,}150Y_i$ (as suggested by plotting N_i^* derived from the Parker relation on Figure 3b), (13) may be solved for Y_{ri}, giving

$$Y_{ri} = 0.42 \qquad (19)$$

This result may also be obtained by using (15) to replace $(N_i/T)_r$ in (16) and solving for Y_{ri}. In both (18) and (19) a condition of partial transport is indicated at reference transport conditions.

If Y_{ri} is known, or predicted from τ_{ri} and D_i/D_{50}, $\tau[50]_i$ may be determined if the form of the Y_i distribution is assumed. In Figure 6b, $\tau[50]_i$ is predicted from the values of Y_{ri} in Figure 6a using a lognormal distribution of $\tau_0/\tau[50]_i$ with mean zero and standard deviation 0.2. For Y_{ri} calculated from (18) the variation of $\tau[50]_i$ with D_i closely follows the fitted values from Figure 1b. The dependence of $\tau[50]_i$ on the assumed shape of the entrainment distribution is not particularly strong; the distribution is merely used to locate $\tau[50]_i$ from a nearby value of Y_{ri}.

Both (17) and (18) (with the former depending only on the assumption that N_i/T is a function of only τ/τ_{ri}) suggest that partial transport prevails at reference transport conditions and that the variation with D_i of Y_{ri} and $\tau[50]_i$ may be predicted as a function of τ_{ri}. Equation (18) provides a specific relation for calculating the degree of partial transport at the reference transport condition. Because observations of q_{bi}, but not of Y_i, are available for other sediments, (18) can be evaluated only in combination with the other transport component relations.

Comparison With the Oak Creek Transport Data

An evaluation of the general applicability of the fractional transport component relations can be made by comparing predicted and observed fractional transport rates for an independent case. The data used for this comparison were collected by *Milhous* [1973] using a vortex sampler on Oak Creek, a small gravel-bed stream in the Oregon coast range. These data provide a useful comparison because of their unusually high quality and because they are well known, having been used by *Parker et al.* [1982] to develop the concept of equal mobility in bed load transport. The Oak Creek data are of particular interest here because, in contrast to BOMC, τ_{rt} varies little with D_i. This provides an opportunity to evaluate the contribution of partial transport to the fractional transport of a sediment for which all sizes are entrained over a narrow range of τ_0.

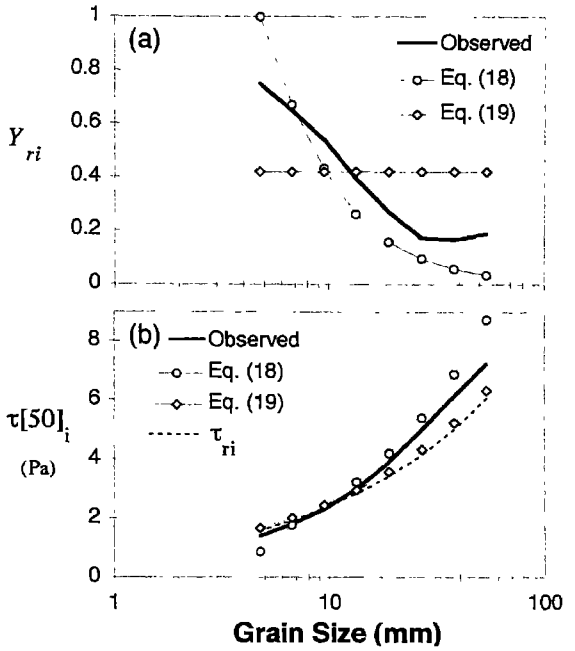

Figure 6. (a) Entrained proportion Y_{ri} of each fraction at the reference shear stress and (b) stress $\tau[50]_i$ mobilizing 50% of the fraction, as a function of grain size. Observed values of Y_{ri} determined using observed values of τ_{ri} and a lognormal $\tau_0/\tau[50]_i$ distribution fitted to the Y_i observations for each grain size [*Wilcock and McArdell*, this issue]. Predicted values of Y_{ri} from (18) and (19), where observed τ_{ri} is used in (18). The prediction using (18) provides a closer fit to the observed values than (19). Reference transport conditions are associated with partial transport of all sizes coarser than D_{50} and Y_{ri} decreases with grain size.

The data used were collected during the winter of 1971, which *Milhous* [1973] indicates are of the best quality. The 22 measurements for discharge $Q > 1$ m^3 s^{-1} are used, which correspond to flow sufficient to break up the bed surface layer and are the same data used by *Parker et al.* [1982]. To facilitate comparison among different flows and provide larger sample sizes, the 22 observations are grouped into six samples with similar q_b (all q_b within a group fall within a factor of 2). Skin friction τ_0 is calculated using the method of *Einstein* [1950]; τ_0 for each group is calculated as a mean weighted by individual sample size.

Transport components and transport rates for Oak Creek data are predicted using, unmodified, the transport component relations developed for BOMC. For each grain size and flow, values of τ_0, τ_{ri}, D_i, and D_{50} must be specified. M_{ai}/F_i is predicted using (6). L_{1i} is predicted using (9) for $D_i > D_{50}$ and using (10) with $\xi = -0.3$ for $D_i < D_{50}$. N_i/T is predicted using (12) with $K = 0.01$. To complete the calculation, values of Y_i and d_x must be predicted. First, Y_{ri} is predicted as a function of τ_{ri} and D_i/D_{50} using (18). The value of $\tau_{ri}/\tau[50]_i$ is found for each Y_{ri} using a lognormal distribution of $\tau_0/\tau[50]_i$ with mean zero and standard deviation 0.2. For $Y_{ri} < 0.5$ the calculation of Y_{ri} is direct. For $Y_{ri} > 0.5$, $\Delta_i = d_x/D_i$ and depends on $D[50]_i$ and therefore on the Y_i distribution, so the solution becomes iterative, although it converges

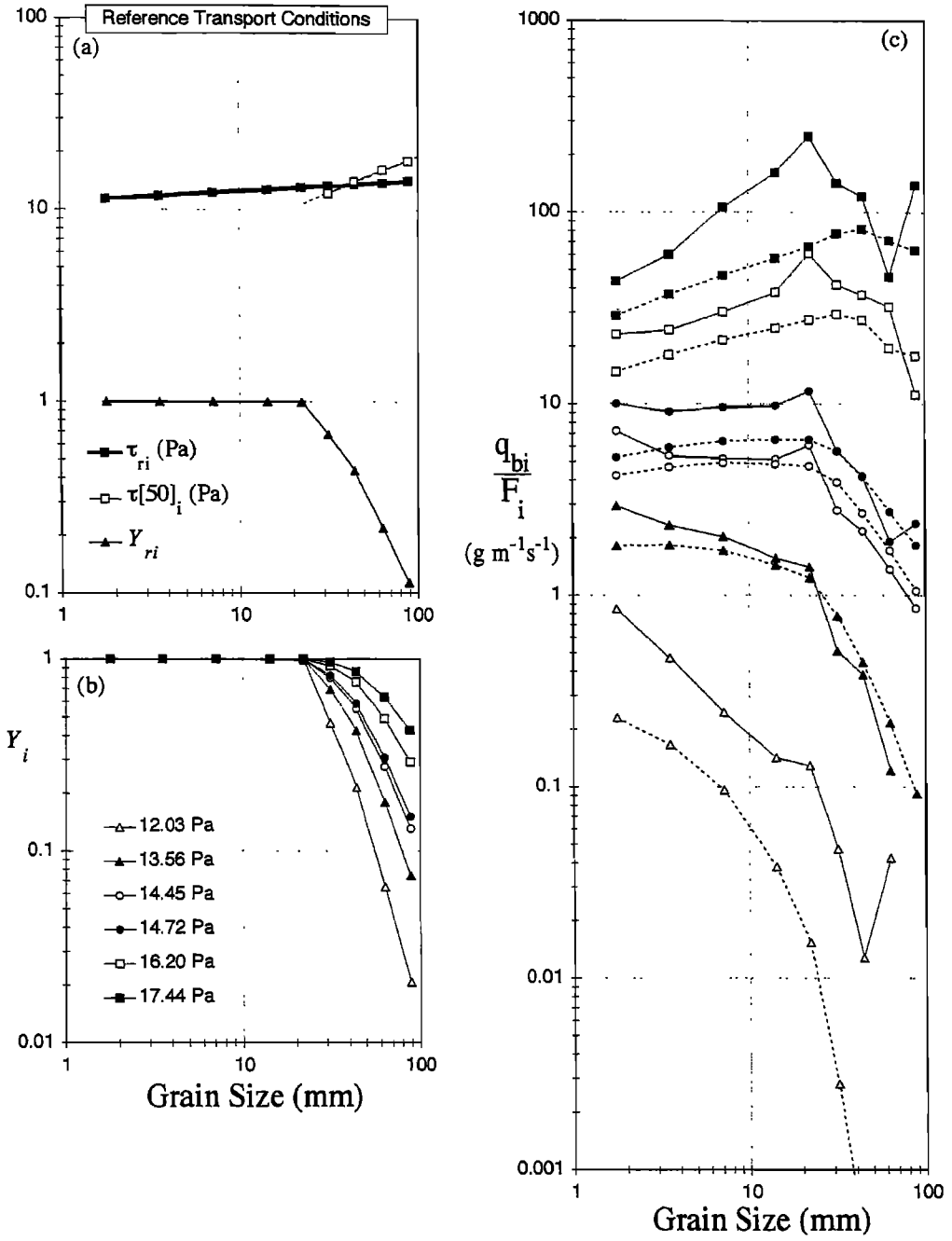

Figure 7. Calculated and observed fractional transport rates for Oak Creek (Winter 1971 data of *Milhous* [1973] grouped into six samples). Calculated values use the transport component relations developed for BOMC, as explained in the text. (a) Reference shear stress τ_{ri}, proportion mobilized Y_{ri} at τ_{ri}, and mean entrainment stress $\tau[50]_i$. Y_{ri} is calculated from τ_{ri} using (18); $\tau[50]_i$ is calculated from τ_{ri} and Y_{ri} using a lognormal distribution of $\tau_0/\tau[50]_i$. The variation of $\tau[50]_i$ with D_i is used to find d_x for each τ_0. (b) Mobile proportion Y_i for each sample. (c) Observed and calculated fractional transport rates. Method of calculation explained in the text. The break in slope of predicted and observed trends match closely, suggesting that partial transport exists even for sediments such as Oak Creek, for which τ_{ri} varies little with grain size. Differences between observed and calculated values may result largely from uncertainty in τ_0; values of τ_0 within 5% of those used give a close match between predicted and observed for all samples.

rapidly because Δ_i is not greatly different from one at the reference transport rate. With $\tau_{ri}/\tau[50]_i$ known for each value of τ_{ri}, $\tau[50]_i$ can be calculated and the value of Y_i for any τ_0 may be found using the lognormal distribution of $\tau_0/\tau[50]_i$. The variation of $\tau[50]_i$ with D_i is also used to give $D[50]_i$ for a specified τ_0. $D[50]_i$ is used as the estimate of d_x.

Values of τ_{ri} for Oak Creek (Figure 7a) were determined by interpolation on plots of q_{bi}/F_i versus τ_0 and may be approximated as $\tau_{ri}/\tau_{r50} = (D_i/D_{50})^{0.057}$ with $\tau^*_{r50} = 0.040$ [*Wilcock*, 1993]. The corresponding values given by *Parker et al.* [1982] are $\tau_{ri}/\tau_{r50} = (D_i/D_{50})^{0.018}$ with $\tau^*_{r50} = 0.088$. The difference in τ^*_{r50} arises because τ_0 has been calculated here

using the form-drag correction of *Einstein* [1950], giving smaller values of τ_0. Because the same values of τ_0 are used to find τ_{ri} and to predict the transport components, the difference is of no immediate significance. The exponent on (D_i/D_{50}) is slightly different because τ_{ri} has been determined by interpolation using additional transport data that extend to values of W_i^* smaller than 0.002 rather than by fitting a loglinear relation of fixed slope through each fraction, as done by *Parker et al.* [1982].

Predicted values of Y_{ri} decrease with grain size for all sizes larger than 25 mm (D_{56}) (Figure 7a). Values of $\tau[50]_i$ are calculated only for fractions with $Y_{ri} < 1.0$. For $Y_{ri} = 1$, $\tau[50]_i$ cannot be reliably found from a probability distribution for Y_i. Values of $\tau[50]_i$ for fractions with $Y_{ri} < 1.0$ span the range of τ_0 for the transport samples, as should typically be the case, so that $D[50]_i$ and d_x for each sample may be found; $\tau[50]_i$ increases more steeply with D_i than does τ_{ri}, following the relation $\tau[50]_i \propto D_i^{0.38}$. The inverse of this relation is used to estimate d_x, which in the form of (5), is

$$d_x/D_{50} = 7968(\tau_{50}^*)^{2.61}$$

where the exponent 2.61 is greater than the value 1.5 in (5), as should be the case when τ_{ri} increases only slightly with D_i. Values of Y_i for each fraction and sample are given in Figure 7b. Partial transport is predicted to exist for all fractions larger than 25 mm (D_{56}) and the magnitude of Y_i increases with τ_0.

The agreement between predicted and observed fractional transport rates (Figure 7c) is remarkably good, considering that the component relations developed for BOMC are applied unmodified to the Oak Creek data. The most significant match is in the shape of the fractional transport curves: the break in slope between fully mobilized and partial transport matches closely for both sets of curves, suggesting the presence of partial transport even though τ_{ri} varies little with grain size.

The agreement between predicted and observed q_{bi}/F_i is best for fractions in the coarse half of the mix ($D_{50} = 20$ mm). These are the fractions for which the transport component relations have been developed and for which partial transport is predicted. For the largest five samples, 41 of the 45 predicted fractional transport rates are within a factor of 2 of the observed values, as are 23 of 25 values for $D_i > 19$ mm. Additional plausible adjustments, particularly in the coefficient and exponent of (12) for $D_i < D_{50}$, could be made to cause the observed and predicted transport rates to match more closely, although such adjustments are beyond the intention of this paper. The separation between predicted and observed fractional transport rates may be attributed to uncertainty in the values of τ_0 used to predict q_{bi}/F_i. Values of τ_0 within 5% of those used cause the predicted and observed trends to overlap for all samples. The influence of uncertainty in τ_0 increases as τ_0 approaches τ_{ri} because of the rapid decrease with τ_0 of both Y_i and N_i/T at small values of τ_0/τ_{ri}.

Conclusions

Fractional transport rate can be expressed as the product of the mass entrainment per unit area, displacement frequency, and displacement length. To account for partial transport of individual size fractions, spatial entrainment is defined relative to the population of grains on the bed surface at some initial time. Partial transport is a condition in which the transport of a fraction is composed of only a portion the surface grains in that fraction, with the remaining grains on the bed surface remaining immobile over the duration of the transport event. Partial transport directly affects the population of grains available for transport and is associated with a rapid decrease in transport rate with increasing grain size, a common feature in gravel-bed rivers.

Approximate relations are developed for each transport component. Observations of the surface concentration and mobile proportion of each fraction are used to estimate spatial entrainment. Displacement length is assumed to increase directly with grain size, as has been found in other studies. Displacement frequency is calculated using the transport component relation with measured values of fractional transport rate and bed surface size distribution. Displacement frequency appears to depend entirely on the bed shear stress τ_0 and the reference shear stress τ_{ri}, which is the value of τ_0 producing a small dimensionless reference transport rate and serves as a surrogate for incipient motion of each fraction. The ratio τ_0/τ_{ri} provides a similarity collapse for displacement frequency for all sizes.

The transport component relations may be used to illustrate the relation between partial transport and fractional transport rates. For fully mobilized fractions (all surface grains entrained at least once), spatial entrainment, scaled by the proportion of each fraction on the bed surface, is independent of grain size D_i. Displacement frequency decreases with D_i and displacement length increases with D_i. The magnitude of these last two components balance, producing fractional transport rates that are independent of D_i. For coarser sizes in the partial transport region (some grains remain immobile over the duration of the run), spatial entrainment decreases rapidly with D_i, taking the same sign as the variation with D_i of displacement frequency, causing the fractional transport rates to decrease rapidly with D_i.

Many models of mixed-size sediment transport are based on a similarity transformation in which the transport relations for each grain size are collapsed to a single curve. The basis for the transformation is the assumption that all size dependence in the fractional transport rates is accounted for by the variation with grain size of the critical shear stress for incipient grain motion. When the transport component relations developed here are combined into such a form, the dimensionless transport is seen to depend on the active proportion of the bed surface Y_i. For sizes in a state of partial transport, Y_i varies with D_i, suggesting that transport similarity does not exist under conditions of partial transport.

Partial transport is a measure of incipient motion based on the proportion of surface grains entrained at least once during a transport event, whereas the reference shear stress τ_{ri} is defined using transport rates, without regard to the source of the grains. Both measures of incipient motion are used in the transport component relations developed here. Because $\tau[50]_i$ is not generally known, whereas τ_{ri} may be measured or estimated, a relation between the two provides a basis for not only predicting the degree of partial transport at the reference transport rate but for calculating the transport components for other sediments. An approximate case is made that partial transport is the general condition at the reference transport rate and that the value of Y_i at τ_{ri} decreases with D_i, even for sediments with a narrow range of τ_{ri}. An explicit relation between Y_i, D_i, and τ_{ri} is developed for the experimental sediment, thereby allowing prediction of Y_i from τ_{ri} and the bed size distribution.

The transport component relations developed for the laboratory case are used, unmodified, to predict the fractional transport rates for Oak Creek, a small gravel-bed river. A reasonably good fit is found between predicted and observed fractional transport rates. Partial transport is predicted to occur for the coarsest half of the sediment, even though all sizes are entrained over a narrow range of τ_0. When plotted as a function of grain size, both predicted and observed fractional transport rates show a similar decrease with grain size, further supporting the conclusion that partial transport occurs for the coarser sizes, even though τ_{ri} varies little with grain size.

The fractional transport component relations presented here do not comprise a complete model for predicting fractional transport rates, primarily because an independent estimate of τ_{ri} is needed to determine the displacement frequency and the mobile proportion of each fraction. Although some empirical [e.g., *Wilcock*, 1993] and theoretical [e.g., *Wiberg and Smith*, 1987] basis exists for estimating τ_{ri}, spatial entrainment, displacement frequency, and transport rate are all sensitive to τ_0/τ_{ri} at values approaching 1 so that uncertainty in either τ_0 or τ_{ri} can produce a large predictive error.

The mobilized proportion of the bed surface is of interest in any problem involving grain sorting between the transport and the bed or size-dependent dispersion of sediment through a river system. With specified values of τ_{ri}, as may be determined with a few observations of flow and transport at small transport rates, the entrainment function proposed here provides a basis for predicting the immobile proportion of the bed surface and its variation with τ_0.

Acknowledgments. Work with the Bed of Many Colors was supported by grant N00014-91-J-1192 from the Office of Naval Research and grants EAR-9004206 and EAR-9205511 from the National Science Foundation. This work benefited from earlier discussions with the Feinstein crew, including Brian McArdell, Chris Paola, Gary Parker, Rebecca Seal, and John Southard. Mike Church, Dave Furbish, Chris Paola, and John Pitlick reviewed an earlier draft of this paper; their thoughtful and perceptive criticisms substantially improved the clarity and completeness of the presentation.

References

Ashida, K., and M. Michine, Study on hydraulic resistance and bedload transport rate in alluvial streams, *Trans. Jpn. Soc. Civ. Eng.*, no. 206, 59–69, 1972.

Church, M., and M. A. Hassan, Size and distance of travel of unconstrained clasts on a streambed, *Water Resour. Res.*, *28*(1), 299–303, 1992.

Drake, T. G., R. L. Shreve, W. E. Dietrich, P. J. Whiting, L. B. Leopold, Bedload transport of fine gravel observed by motion-picture photography, *J. Fluid Mech.*, *192*, 193–217, 1988.

Einstein, H. A., Bedload transport as a probability problem (in German), Ph.D. thesis, ETH, Zurich, 1937. (Translation by W. W. Sayre in *Sedimentation*, Appendix C, edited by H.-W. Shen, pp. C1-C105, Colo. State Univ., Fort Collins, 1972.)

Einstein, H. A., The bedload function for sediment transport in open channel flows, *Tech. Bull. 1026*, Soil Conserv. Serv., U.S. Dep. of Agric., Washington, D. C., Sept. 1950.

Emmett, W. W., R. L. Burrows, and E. F. Chacho Jr., Coarse particle transport in a gravel-bed river, paper presented at International Workshop on Gravel-Bed Rivers: Dynamics of Gravel-Bed Rivers, Florence, Italy, Sept., 1990.

Fernandez Luque, R., and R. van Beek, Erosion and transport of bedload sediment, *J. Hydraul. Res.*, *14*(2), 127–144, 1976.

Haschenburger, J. K., Scour and fill in a gravel-bed channel: Observations and stochastic models, Ph.D. Thesis, 144 pp., Univ. of British Columbia, Vancouver, Canada, 1996.

Hassan, M. A., and M. Church, The movement of individual grains on the streambed, in *Dynamics of Gravel-Bed Rivers*, edited by P. Billi, R. D. Hey, C. R. Thorne, and P. Tacconi, John Wiley, New York, 1992.

Hassan, M. A., M. Church, and P. J. Ashworth, Virtual rate and mean distance of travel of individual clasts in gravel-bed channels, *Earth Surf. Processes Landforms*, *17*, 617–627, 1992.

Milhous, R. T., Sediment transport in a gravel-bottomed stream, Ph.D. thesis, Oregon State Univ., Corvallis, 1973.

Nakagawa, H., T. Tsujimoto, and H. Miyamoto, 16mm film analysis of characteristic quantities of bed load transport (in Japanese), *Annals*, vol. 21B-2, pp. 407–421, Disaster Prev. Res. Inst., Kyoto Univ., Kyoto, Japan, 1978.

Nakagawa, H., T. Tsujimoto, and Y. Hosokawa, Statistical mechanics of bed-load transportation with 16mm film analysis of behaviors of individual sediment particles on a flat bed, paper presented at Third International Symposium on Stochastic Hydraulics, Int. Assoc. Hydraul. Res., Tokyo, 1980.

Nakagawa, H., T. Tsujimoto, and S. Nakano, Characteristics of sediment motion for respective grain sizes of sand mixtures, *Bull. Disaster Prev. Res. Inst., Kyoto Univ.*, *32*(1), 1–32, 1982.

Nelson, J. M., R. L. Shreve, S. R. McLean, and T. G. Drake, Role of near-bed turbulence in bed load transport and bed form mechanics, *Water Resour. Res.*, *31*(8), 2071–2086, 1995.

Parker, G., Hydraulic geometry of active gravel rivers, *J. Hydraul. Div. Am. Soc. Civ. Eng.*, *105*(HY9), 1185–1201, 1979.

Parker, G., P. C. Klingeman, and D. L. McLean, Bedload and size distribution in paved gravel-bed streams, *J. Hydraul. Div. Am. Soc. Civ. Eng.*, *108*(HY4), 544–571, 1982.

Schmidt, K.-H., and P. Ergenzinger, Bedload entrainment, travel lengths, step lengths, rest periods—studied with passive (iron, magnetic) and active (radio) tracer techniques, *Earth Surf. Processes Landforms*, *17*, 147–165, 1992.

Stelczer, K., *Bedload Transport: Theory and Practice*, 295 pp., Water Resour. Publ., Littleton, Colo., 1981.

Wiberg, P. L., and J. D. Smith, Calculations of the critical shear stress for motion of uniform and heterogeneous sediments, *Water Resour. Res.*, *23*, 1471–1480, 1987.

Wilcock, P. R., The critical shear stress of natural sediments, *J. Hydraul. Eng.*, *119*(4), 491–505, 1993.

Wilcock, P. R., and B. W. McArdell, Surface-based fractional transport rates: mobilization thresholds and partial transport of a sand-gravel sediment, *Water Resour. Res.*, *29*(4), 1297–1312, 1993.

Wilcock, P. R. and B. W. McArdell, Partial transport of a sand/gravel sediment, *Water Resour. Res.*, this issue.

Wilcock, P. R., A. F. Barta, C. C. Shea, G. M. Kondolf, W. V. G. Matthews, and J. C. Pitlick, Observations of flow and sediment entrainment on a large gravel-bed river, *Water Resour. Res.*, *32*(9), 2897–2909, 1996.

P. Wilcock, Department of Geography and Environmental Engineering, Johns Hopkins University, Baltimore, MD 21218. (e-mail: wilcock@jhu.edu)

(Received April 15, 1996; revised August 26, 1996;
accepted August 28, 1996.)